

Active 433 MHz-W UHF RF-powered chip integrated with a nanocomposite *m*-MWCNT/polypyrrole sensor for wireless monitoring of volatile anesthetic agent sevoflurane

Murthy Chavali^{a,*}, Tzu-Hsuan Lin^b, Ren-Jang Wu^{c,**}, Hsiang-Ning Luk^d, Shih-Lin Hung^b

^a Environmental Techniques Center, U-CAN DynaTex Inc., No. 95 Nankang 3rd Road, Nankang Industrial Park, Nantou City 540, Taiwan, ROC

^b Department of Civil Engineering, National Chiao Tung University, Ta Hsueh Road, Hsinchu 300, Taiwan, ROC

^c Department of Applied Chemistry, Providence University, Shalu, Taichung Hsien 433, Taiwan, ROC

^d Department of Anesthesia, Taichung Veterans General Hospital, Taichung Harbor Road, Taichung 407, Taiwan, ROC

Received 20 October 2006; received in revised form 2 May 2007; accepted 3 July 2007

Available online 10 July 2007

Abstract

Tiny remote sensors capable of monitoring gases and vapors are having greatest demand due to their potential applications in diverse research fields. In the present work, design and fabrication of an active wireless UHF (433 MHz) RF-powered sensing system for monitoring volatile organic compounds is presented. The developed sensor chip consists of a thin film of gas-responsive composite material, based on modified multiwalled carbon nanotubes (*m*-MWCNTs) and polypyrrole (Ppy), coated over two comb-like interdigitated gold electrodes. Wireless modules have been integrated with the chemical sensor chip (composite *m*-MWCNTs/Ppy) and RF components to detect volatile anesthetic agent, fluoromethyl 2,2,2-trifluoro-1-(trifluoromethyl) ethyl ether (sevoflurane) is demonstrated.

© 2007 Elsevier B.V. All rights reserved.

Keywords: Wireless; RF sensor; Sevoflurane; Fluoromethyl 2,2,2-trifluoro-1-(trifluoromethyl) ethyl ether; Ultane; Polypyrrole; MWCNT; *m*-MWCNT; Chemical sensor

1. Introduction

Demand for tiny, accurate and reliable sensors capable of monitoring gases and vapors is growing multifold due to their potential applications in food sector, quality control, medical, soil monitoring [1] and towards environmental pollutants [2]. In the past several pilot studies and on field-testing suggested that wireless sensor technology (*both passive and active*) can reduce the installation cost by no less than tenfold, making it a more attractive option for end users to install [3]. Portability and wireless data connectivity made these sensors more competitive and advantageous, in particular when sensors are to be deployed in harsh environments.

Monitoring gaseous analytes [including vapors] inside a sealed environment, like food packages, huge storage containers [4], closed buildings, clean rooms, hospitals, etc. is important, prompting development of wireless sensor technologies. In the present days radio-tagged technology is combined with several sensor systems—temperature, humidity, strain and pressure sensing, or simultaneously monitoring of any of these, temperature and pressure [5] and even extended towards monitoring environmental pollutants [6], smart dust sensors [7], bio-implantable devices [8], etc. For example, hospital surgical wards use numerous inhalational anesthetic agents nearly all of them are harmful volatile liquids of halogenated derivatives of alkanes. The commonest of them is fluoromethyl 2,2,2-trifluoro-1-(trifluoromethyl) ethyl ether commercially known as *sevoflurane* (C₄H₃F₇O; 1990 as *Ultane*; Fig. 1), play a crucial part in pain management of patients undergoing surgery [9,10]. The exposure to left over volatile anesthetic agent is also unsafe for those working in operating rooms, dental offices, and veterinary offices. Measuring the concentration of sevoflurane in blood and in clinical inhalation has now become important. Reports

* Corresponding author. Tel.: +886 49 2260848x28; fax: +886 49 2260849.

** Corresponding author. Tel.: +886 4 26328001 15212; fax: +886 4 26327554.

E-mail addresses: ChavaliM@gmail.com (M. Chavali), rjwu@pu.edu.tw (R.-J. Wu).

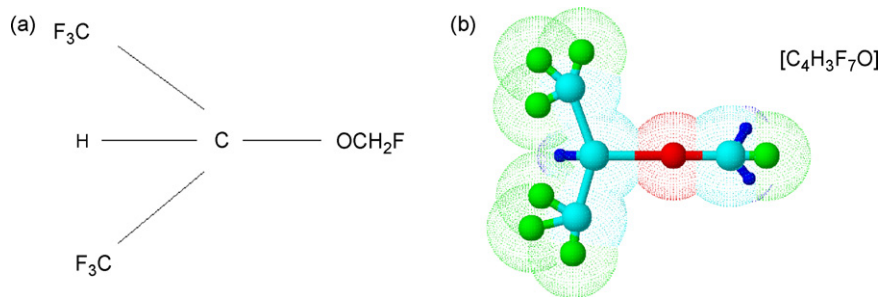


Fig. 1. Sevoflurane, fluoromethyl 2,2,2-trifluoro-1-(trifluoromethyl) ethyl ether: (a) Chemical structure and (b) 3D model.

also mentioned that some of the highest levels of waste anesthetic gases have been found in post-operative recovery rooms [11] affecting the non-surgical staff.

Advanced measurement techniques like, gas chromatography (GC) either in combination with methods like GC–mass spectrometry (GC–MS) are applied for detecting of the concentration of sevoflurane in blood [12]. Ho and co-workers [13] further modified the previously developed headspace (HS) GC–MS method to analyze and distinguish simultaneously the five common clinical inhalation anesthetics that includes sevoflurane. Infrared (IR) method [14] was used to measure the concentration of sevoflurane in inhalation and expiration of patient's breath. Floate and Hahn [15] used the electrochemical reduction method to detect the sevoflurane both at low concentrations ($[\text{sevoflurane}] < 0.2\%$, v/v) and high concentrations ($0.5 < [\text{sevoflurane}] < 2\%$, v/v). Reverse-phase high-performance liquid chromatography (RP-HPLC) was applied for estimating sevoflurane indirectly by measuring the urinary metabolite, hexafluoroisopropanol (HFIP) [16]. The limit of detection obtained for HFIP using RP-HPLC was close to $1 \mu\text{g/L}$ level. Other groups used high-resolution two-dimensional (HR2D) Fluorine-19 NMR to determine sevoflurane [17].

Ability to monitor and detect volatiles using low-cost devices has been shown to be challenging in many applications [18]. Of these monitoring systems, polymer-based sensors, such as carbon black–polymer composite [19], polymer-coated quartz crystal microbalances (QCM) [20], polymer-coated surface acoustic wave (SAW) devices [21], and sensors based on conducting polymer composites [22], have an advantage to operate at room temperature whilst consuming low power. Conducting polymers offer themselves as an excellent sensing materials [23], among the many, polypyrrole (Ppy) is the most extensively used in the designing materials for chemical gas sensors [24]. Versatility of this polymer is determined by a number of potential applications: strong absorptive properties towards gases [25], DNA [26], proteins [27], catalytic activity [28] and, corrosion protection properties [29], etc. Ppy and Ppy doped with copper films revealed increasing the resistance by exposure of reducing gases such NH_3 , H_2 and CO [30]. Blending Ppy with either poly(caprolactone), poly(ethylene oxide), poly(methyl methacrylate), poly(vinyl alcohol) or poly(vinyl acetate) exhibited sensitivity to methanol, ethanol, carbon tetrachloride and benzene [31]. Carbon nanotubes (CNTs) have recently found applications both as sensors [32] and actuators [33]. CNTs and conducting polymer composites were also

reported as sensors, like CNT/Ppy [34] based sensors and Ppy-based electronic nose [35] were applied for measuring NH_3 , NO_x , CO , SO_2 , H_2S , CH_4 , O_2 , H_2 , EtOH , $\text{C}_6\text{H}_5\text{OH}$, C_6H_6 and $\text{H}_2\text{O}_{(\text{vapor})}$.

The objectives of this work were to report on design and development of an active UHF-5 (433 MHz) wireless RF sensor for the detection of anesthetic agent, sevoflurane and examine the performance this low-cost device. Sensing film was a composite material made of *modified*-MWCNT/polypyrrole, developed by *in situ* UV-photo polymerization. Films were then deposited by means of dip coating over two comb-like interdigitated gold electrodes screen-printed on an alumina chip substrate. By integrating RF components to chemical sensor chips for monitoring of volatiles like sevoflurane can be done wirelessly. Here in this paper all the required RF system components for the sensor operation were discussed. Among the passive and active types of wireless sensors, passive type are without an internal power supply which could literally extend lifetime of the hardware RF components at the same time minimizing the overall cost factor. Though this is possible, here we have focused on the development of low-cost, active wireless sensors that are desired and could readily be used on a disposable basis.

2. Sensor design and overview

The wireless sensor architecture described here depends on power nodes operating with a single, microprocessor base station and single or a few distributed wireless sensors. Network architecture and communication protocols are developed to exploit the asymmetry of distributed sensor communication. Distinctively, most information flow is from the sensor nodes to the base station with considerably less flow in the form of commands to the sensor nodes from the base station. A schematic of the proposed wireless gas sensor system is given in Fig. 2. The overall system design comprises of two major units, a wireless sensing unit and a wireless receiving unit. The sensing system includes sensor chip, data acquisition module (MDA500), a microprocessor with wireless RF module (MICA2DOT) and a gateway (MIB510, Crossbow Technology Inc., CA, USA; <http://www.xbow.com/>) and a host computer. The data acquisition module can log the data from sensor chip. The microprocessor on the sensing unit is primarily used to acquire the signal from the data acquisition module, while on the receiving unit, the microprocessor processes the received data to the gateway connected with host PC. The transmission

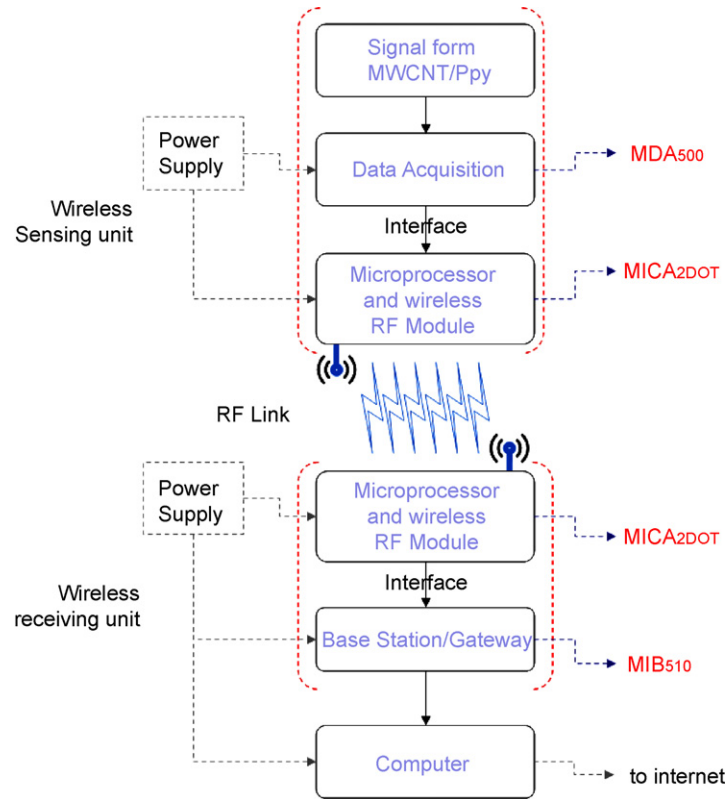


Fig. 2. Schematic of the wireless gas sensor measurement system.

data between sensing and receiving units were transmitted via wireless RF module.

2.1. Hardware

The proposed setup was capable of both sensing and receiving the signal originating for their respective units wirelessly. Within the existing architectural plan, the wireless sensing unit contains two functional modules, (1) sensing and data acquisition module; (2) microprocessor with wireless communication module. Furthermore, the wireless receiving unit design also consists of two functional modules, a microprocessor with wireless communication module and a gateway. Fig. 3 is the graphic design of the wireless sensing unit and wireless receiving unit with predefined essential electrical components.

The sensing and data acquisition module MDA500 provides a flexible user-interface for linking external signals to the MICA2DOT (MPR510) mote that serving as both microprocessor and wireless communication module. Each MDA500 channel was used to take the signals and convert them into well-digitized voltage output ranging from 0 to 3 V. The hardware specifications of MICA2DOT are listed in Table 1. All the major I/O signals of the MICA2DOT mote are compatible with the MDA500 circuit board. The data from MDA500 is processed by an on-board low power consuming micro-controller Atmega128 (Atmel Corporation, San Jose, CA) with 512KB flash memory.

The MICA2DOT has six input channels, each with its own 10-bit ADC. The architecture of the sensor allows the addition of other transducers without alteration of the telemetry chan-

nel or significant changes to the sensor design. The 18 pins on MICA2DOT are used for connecting six analog inputs, digital I/O, and a serial communication or UART interface making it easy to connect to a wide variety of external sensors and devices. The MICA2DOT mote uses the same hardware as the MICA2, but much smaller in size (MICA2 is 58 mm × 32 mm × 15 mm). The shape of MICA2DOT is circular, diameter of 25 mm, and

Table 1
Microprocessor and wireless communication module hardware specifications

Component	Attribute	Specification
MCU	Chip	ATmega128L
	Type	4 MHz, 8 bit
	Program memory (KB)	128
	SRAM (KB)	4
Sensor board interface	Type	18 pin
	10 bit ADC	6 inputs, 0–3 V
	UART	1
	Other interface	DIO
Radio	Chip	CC1000
	Frequency (MHZ)	433
	Data rate (kbit/s)	38.4
	Antenna connector	PCB solder hole
Fragsh data logger memory	Chip	AT45DB014B
	Connector type	SPI
	Size (KB)	512
Power Source	Type	Coin (CR2354)
	Capacity (ma/hr)	560

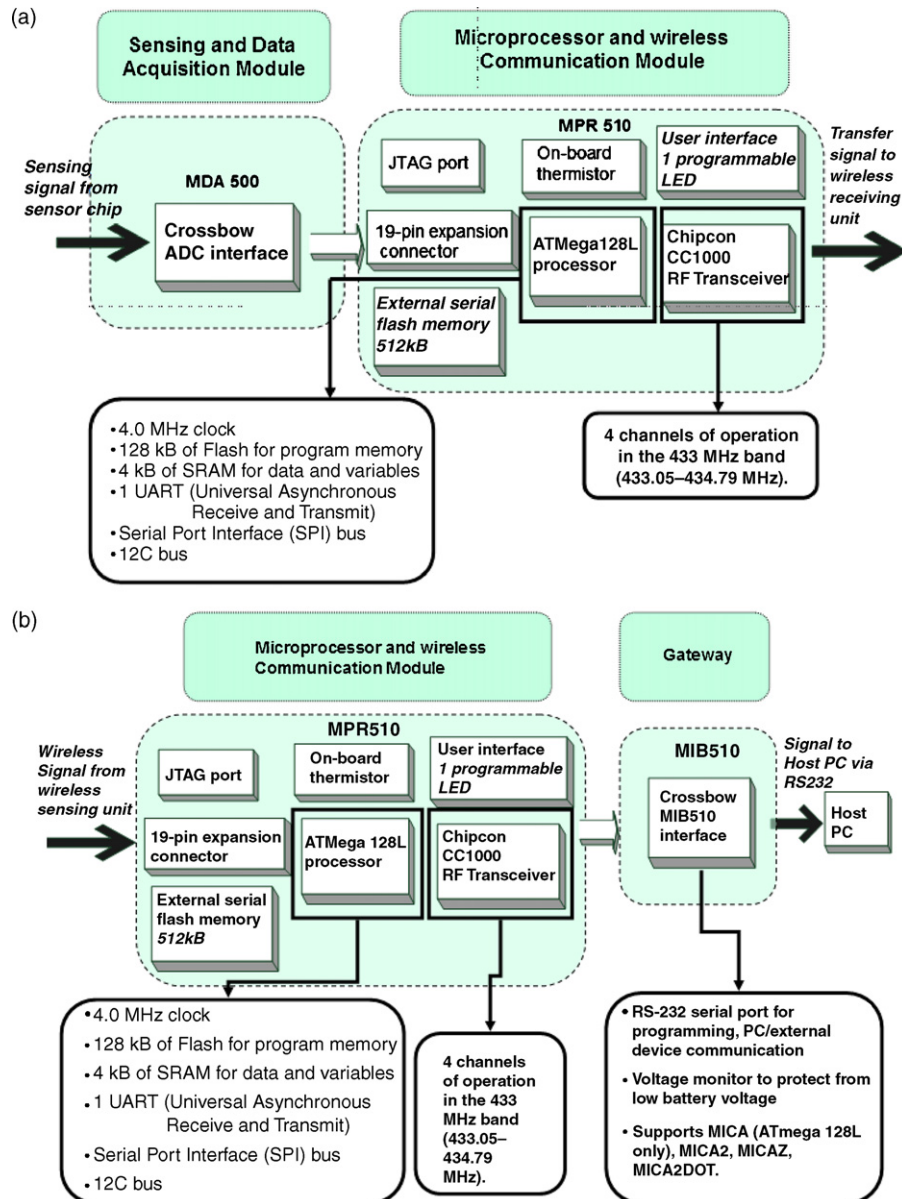


Fig. 3. System architecture contains (a) wireless sensing unit with two functional modules, for sensing, data acquisition and microprocessor with wireless communication module. (b) Wireless receiving unit with two functional modules, for microprocessor with wireless communication module and gateway.

its thickness was approximately 6 mm. The wireless data transmission between the MICA2DOTs was linked to a RF radio chip (CC1000, Chipcon AS, Oslo, Norway) via FSK. The distance between the transmitter and receiver in our measurements was over two meters. The RF chip, Chipcon CC1000 FSK-modulated radio uses MPR510 (433 MHz) in this system. With regard to the MIB510 gateway is connected to a host PC. This interface board is used to allow the motes to communicate with a PC, and is compatible with the MICA2DOT and has operates on external power supply. The device provides an interface for RS232 serial port and reprogramming port that can download the codes into an on-board in-system processor via RS232 serial port. The system can also enable uploading the sensor readings directly, making them available online. As a result, any user can access these sensor readings over Internet.

2.2. Software

MICA2DOT platform runs on a component-based runtime environment called TinyOS (University of California, Berkeley) that has been specifically written to implement data-acquisition and wireless MAC protocols for the MICA2DOT transmitter. TinyOS has component library for network protocols, distributed services, sensor drivers and data acquisition tools. This library allows the user to construct easily the individual application. The standard software to program in TinyOS is the “ μ In-System Programmer” (UISP). The TinyOS supports a variety of device programmers, including any standard parallel-port programmer board, serial port-based programming device, the Atmel AVRISP, the Ethernet Programming Board (EPRB). In this work, the MIB510 was used to be the serial port-based pro-

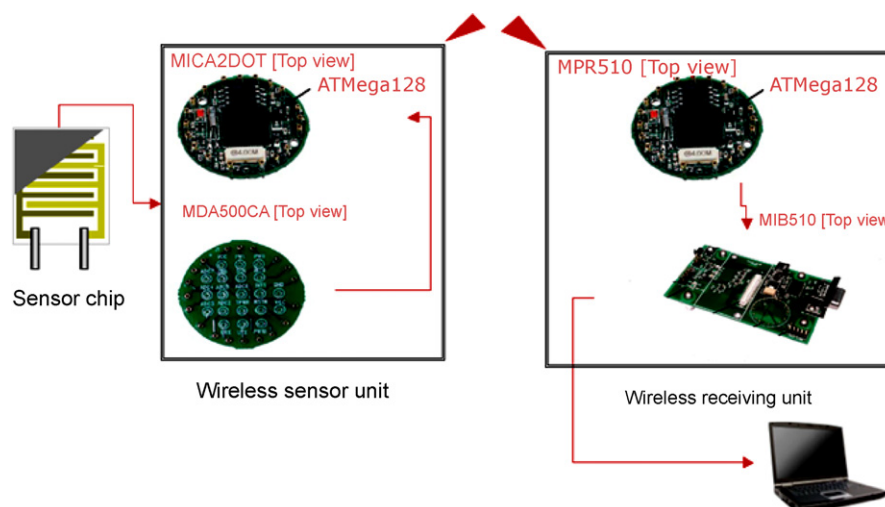


Fig. 4. Architecture of wireless system and sensor chip integration.

gramming device. The TinyOS system is written in nesC, which is a new C-like syntax language for wireless sensor networks. In fact, the TinyOS-enabled MICA2DOT grants high-level applications with direct and efficient control over low-level hardware, making it easy for developers' application specific high-level networking and communication protocols.

2.3. Sensor chip integration

The architecture of this integrated wireless system is shown in Fig. 4. The sensing system integrates several units, like, a sensor chip, a wireless sensing unit and a wireless receiving unit. The sensor chip is fabricated by coating the Ppy thin film over the chip; the details of materials and methodology given under experimental part. Within this architecture, the sensor chip is connected to the wireless sensing unit. Once the sensor chip acquires the signal from environment, the change in resistance of the sensor chip is converted to change in voltage with the help of a simple circuit that was connected to the data acquisition module. After that, the microprocessor and wireless communication module sends the signal to the wireless receiving unit. Upon sensing, the signal is transmitted to the host PC via RS232 serial port directly. The functions of all components in this system are presented in Table 2.

Table 2
Function of all components in wireless sensing system

Unit	Component	Function
Sensor chip	Sensing film	Sensing the signal from environment
Wireless sensor unit	MDA500	Analog to digital interface
	MPR510	Processing signal and transiting signal wirelessly
Wireless sensor unit	MPR510	Processing signal and receiving signal wirelessly
	MIB510	Programming the microprocessor, to serve as a gateway and base-station

2.4. Data acquisition and transmission

The Data acquisition Module is MDA500 (Crossbow Technology Inc., CA, USA; <http://www.xbow.com/>), which provides a flexible user-interface for connecting external signals to the MICA2DOT mote. All of the major I/O signals of the MICA2DOT mote are routed to plated-through socket depths located over the MDA500 circuit board. MICA2DOT (Crossbow Technology Inc., CA, USA; <http://www.xbow.com/>) mote serves as the Microprocessor and Wireless Communication Module. The MICA2DOT, MPR510 (433 MHz), was used in this system. The Motes use the Chipcon CC1000 FSK-modulated radio. The components of data acquisition and transmission are shown in Fig. 5. Fe models utilize a powerful ATmega 128L microcontroller and a frequency tunable radio with extended range. The MPR4x0 and MPR5x0 radios are compatible and can communicate with each other as long as the "x" is the same number.

2.5. Host PC

MIB510 (Crossbow Technology, Inc., CA, USA; <http://www.xbow.com/>) that we used was connected to a laptop as a Host PC. The MIB510 interface board is a multi-purpose interface board used with the MICA2DOT Mote. It supplies power to these devices through an external power adapter option, and provides an interface for a RS-232 Mote serial port and reprogramming port. The MIB510 has an on-board in-system processor (ISP) – an Atmega16L – to program the Motes. Code was downloaded to the ISP through the RS-232 serial port and then the ISP program the code into the mote.

3. Experimental part

3.1. Materials and equipment

All the chemicals were of analytical grade purity, AR (>99%), and were used as provided from Sigma–Aldrich Inc. USA with-

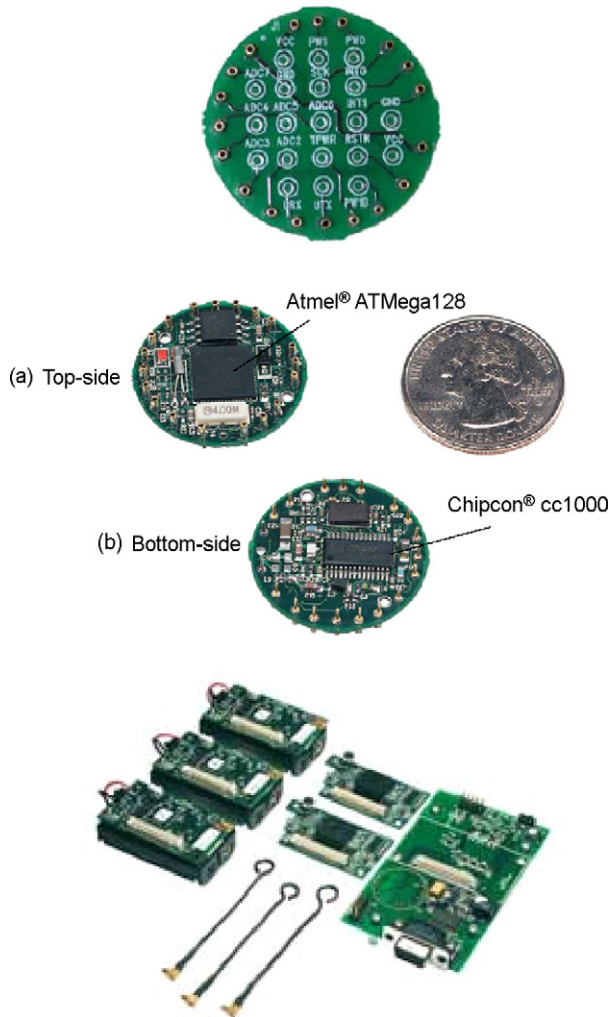


Fig. 5. The RF system components for data acquisition and transmission.

out any further purification, monomer pyrrole (Py) was distilled under reduced pressure and stored in a desiccator below 4 °C to be used. Distilled and deionized (DI) water was used, where required. Water for samples and standards preparation was purified with Milli Q-purified (Millipore Milli Q185 Plus system, Millipore, USA). The MWCNTs were synthesized in the laboratory. Sevoflurane (*Ultane*) used in this work was provided by Abbott Laboratories, U.K. (<http://www.abbott.com/>).

Polymerization process of Ppy was studied using a UV–vis spectrophotometer, SINCO, SUV-2100 series (<http://www.scinco.com>; Korea) and IR characterization of sevoflurane was done with ABB-BOMEM FTIR (D8 Series, Canada) equipped with a mercury–cadmium–telluride (MCT) detector. NaCl crystals of dimensions 25 mm in diameter and thickness of 4 mm (Spectral Systems Inc., #955–3616; USA) were used as stage for collecting sevoflurane spectrum.

3.2. MWCNTs synthesis and acid treatment

Multiwalled CNTs (MWCNTs, Seed Chem CN3001) were used in the preparation of composite polypyrrole films after modification. The MWCNTs were chemically synthesized by

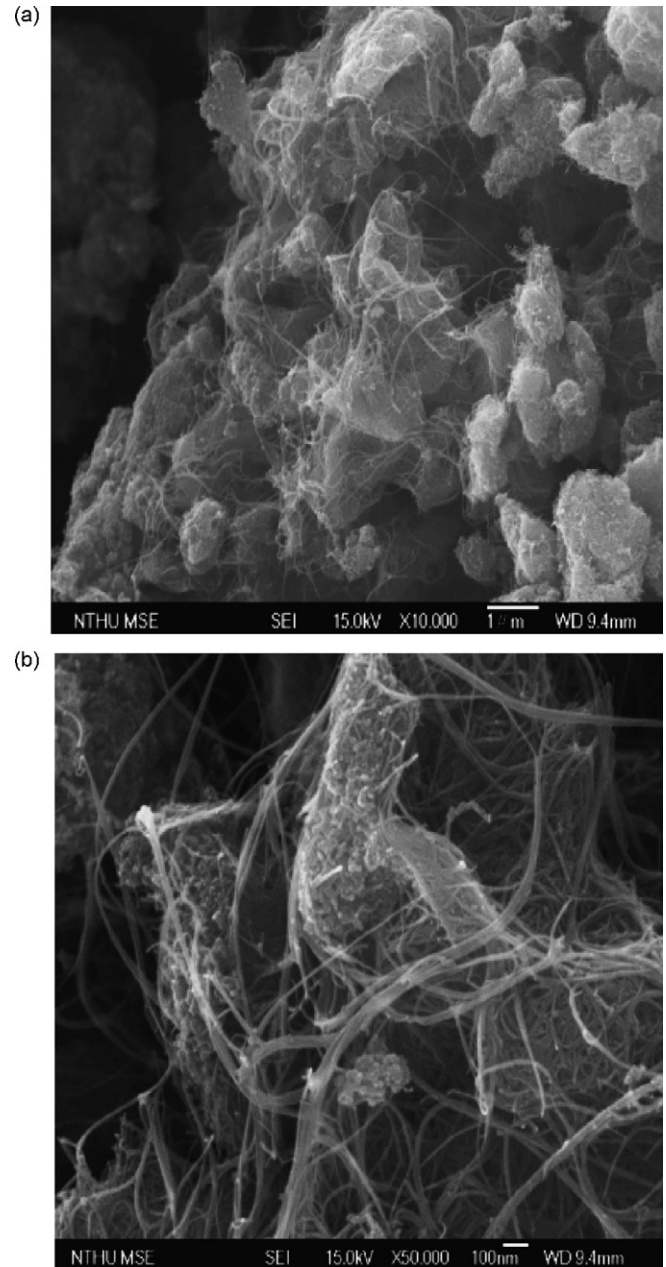


Fig. 6. FE-SEM images of as prepared MWCNTs: (a) magnification of 10,000× and (b) magnification of 50,000×.

the liquid–liquid solution (L–L–S) method at Material Chemical Laboratories, Industrial Technology Research Institute (MCL/ITRI) of Taiwan, ROC. Synthesized MWCNTs (150 mesh) have flocculent nanopowder texture (Fig. 6) and they are highly size controllable, having purity <95% and high aspect ratios (length, 500 μm to diameter, <10 nm). The average pore volume was around 0.8 cm³/g, density ~2.1 g/cm³, and the special surface area of 40–300 m²/g. The obtained MWCNTs were with closed ends.

Further, the MWCNTs were modified in order to open the ends by aggressive break opening (the closed ends) with acid treatment. Prior to acid treatment MWCNTs underwent hydrolysis by sonicating in DI water for 16 h. Subsequently they were

treated with acid (3:1, Conc. HCl to Conc. HNO₃) for 36 h while under sonication. The products were filtered and dried in the oven at 200 °C for approximately 2 h. The modified MWCNTs (*m*-MWCNTs) have now open ends and are ready to be blended with pyrrole for preparing *m*-MWCNTs/Ppy nanocomposite films (prepared by *in situ* UV photo polymerization) that will sense sevoflurane.

3.3. Synthesis of *m*-MWCNTs/Ppy composite thin films

Composite *m*-MWCNT/Ppy films were prepared by *in situ* UV photo polymerization method [36] described elsewhere, polymerizing together monomer Py and AgNO₃ that acts as an initiator. 3.354 g of monomer Py were mixed with 50 ml of EtOH, approximately AgNO₃ of 1 wt.% of Py and 1 wt.% of *m*-MWCNT of Py were added to the solution and homogenized. This mixture solution containing the monomer, Py and AgNO₃ was UV photo irradiated for 5.5 h. The polymerization process was confirmed by the UV–vis spectroscopy. An alumina chip with dimensions of 10 by 5 mm comprising of a pair of comb-like interdigitated gold electrodes previously screen printed over the substrate was used to dip coat Ppy thin films as shown in Fig. 7. The ends of the gold electrodes were connected to the wiring through platinum electrodes. The addition of *m*-MWCNT to Ppy film was mainly to enhance the sensitivity.

3.4. Chemical sensor setup

A dynamic flow system for the sevoflurane-sensing chamber was used as depicted in Fig. 8. Several concentrations of sevoflurane were prepared using the divided flow method and two mass flow controllers (MFCs) were used to tune the dilution factor. Within the test system, the concentration varied from 0.1% to 10%. The flow rate of the test gas was fixed at 1000 cm³/min dur-

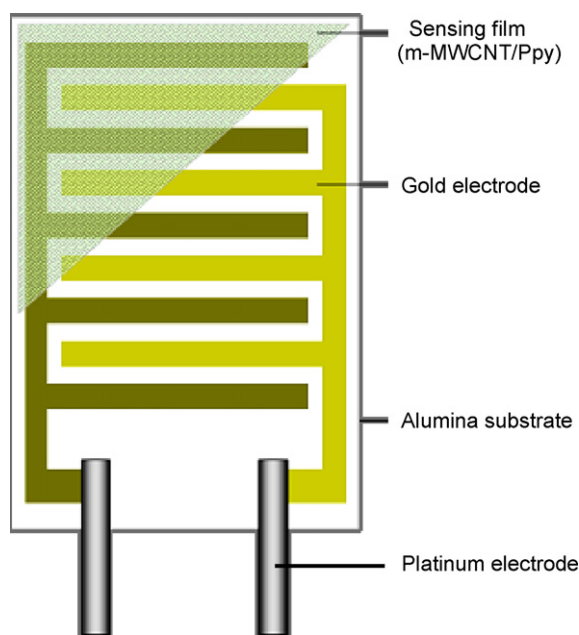


Fig. 7. Top view of the *m*-MWCNT/Ppy sensor chip.

ing the measurements. A simple voltage circuit was designed in order to facilitate measurements (Fig. 9). V_s , input voltage ($V_s = 2.0$ V), the cascade sensor head resistance is R_s , and the reference resistance is R_r . The input data consists of the voltage difference (V_m) across the reference resistance. The sensor resistance and response (S) can be obtained from Eqs. (1) to (5):

$$I = \frac{V_s}{R_s + R_r} = \frac{V_m}{R_r} \tag{1}$$

$$R_s = R_r \frac{V_s - V_m}{V_m} \tag{2}$$

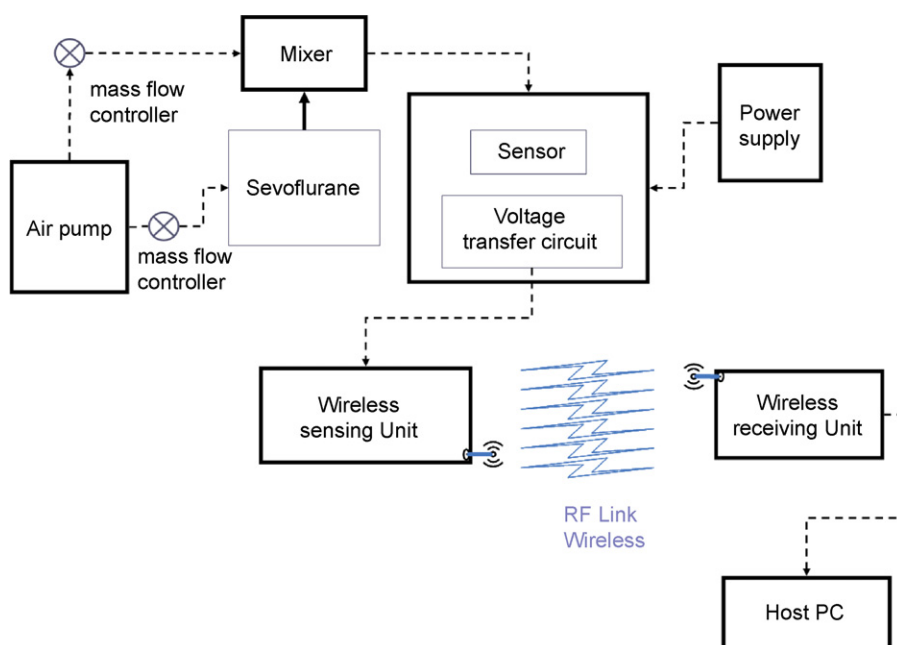


Fig. 8. Experiment setup of wireless gas sensor measurement system.

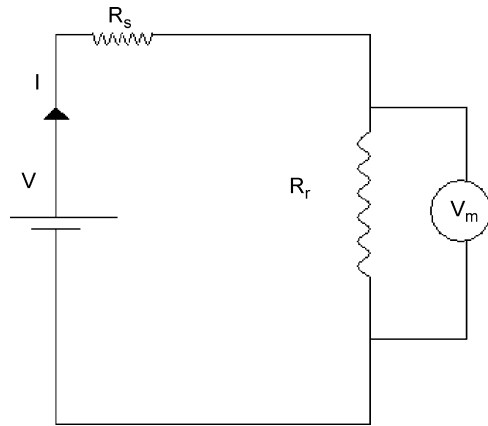


Fig. 9. Voltage measuring electrical circuit of *m*-MWCNTs/Ppy sensors.

$$R_{\text{Air}} = R_r \frac{V_s - V_{\text{Air}}}{V_{\text{Air}}} \quad (3)$$

$$R_{\text{Gas}} = R_r \frac{V_s - V_{\text{Gas}}}{V_{\text{Gas}}} \quad (4)$$

$$S = \frac{R_{\text{Gas}}}{R_{\text{Air}}} = \frac{V_{\text{Air}}(V_s - V_{\text{Gas}})}{V_{\text{Gas}}(V_s - V_{\text{Air}})} \quad (5)$$

All the sensing experiments were developed at temperature 24.5 ± 0.5 °C, and humidity was kept at $60 \pm 5\%$ RH.

The wireless sevoflurane sensor setup is shown in Fig. 6. The alumina chip placed inside a test chamber is connected to the wireless sensing unit via a voltage circuit. The simple circuit is designed to transfer the measure signal from resistance to voltage. Test gas concentration was controlled using two mass flow controllers (MFCs), which subsequently maintains the required flow rate of the test gas that was equivalent to the required concentration during measurement. One of the MFCs control the flow rate of dry air and another was used to secure volatile sevoflurane. The flow rate of the test gas was fixed at $1000 \text{ cm}^3/\text{min}$ during the measurements. Dry air and volatile sevoflurane were mixed thoroughly in the mixing chamber before they were directed towards the sensor chip. Once the gas is in contact with the sensor chip, there is a change in signal (either resistance or voltage) corresponding to the concentration of sevoflurane. The resistance changing will be transformed to voltage via the circuit. Subsequently, the connected RF sensing unit transmits the signal to a RF receiving unit that was connected to a host PC.

4. Preliminary results and discussion

4.1. Py and Ppy UV-vis spectra

Ppy sensing material was synthesized by *in situ* UV photo-polymerization of pyrrole, and dip coated on the sensor chip with dimensions of 10 mm by 5 mm with a pair of comb-like interdigitated gold electrodes were screen printed on it. UV-VIS spectrum of pyrrole was given in Fig. 10 and the peak of pyrrole band was at 280 nm; after UV treatment at room temperature for 5.30 h for photo-polymerization [37] occurs and broad peaks

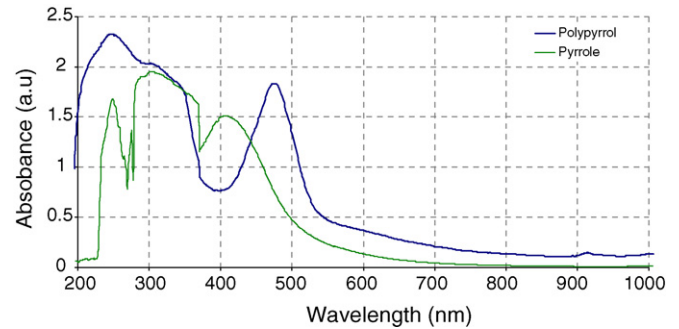
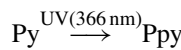


Fig. 10. UV-vis spectrum of Py and photo-polymerized Ppy.

were seen over a range of 350–450 nm indicating the completion of polymerization:



This explains how pyrrole monomers were polymerized into polypyrrole. Thus obtained prominent absorption peak at 440 nm is due to the electronic transition of π to π^* bonds in Ppy [38].

4.2. FTIR characterization of sevoflurane

A typical infrared (IR) spectrum of the sevoflurane was recorded on a NaCl crystal. Most of the obtained vibrational bands were identified from the FTIR spectrum in relevance with that of the available literature. The FTIR spectrum of sevoflurane vapor was collected at room temperature in transmission mode from 500 to 3200 cm^{-1} . Interpretation of FTIR spectrum is done by correlating the absorption bands in the measured spectrum with the known absorption frequencies for types of bonds thus followed with these observations. In case of sevoflurane all we except is aliphatic stretching frequencies. The obtained IR spectrum have several prominent bands in the region 1033 – 1378 cm^{-1} and few less significant bands in the region 2100 – 3000 cm^{-1} , which mostly comprise aliphatic stretching frequencies of $-\text{CH}$, $-\text{CH}_2$, $-\text{CH}_3$ and the spectrum is having all the expected characteristic peaks like, stretching frequencies from $-\text{CF}$, ν_{CF} mostly form between 1100 and 1400 cm^{-1} . Below 1000 cm^{-1} there are three prominent peaks at 692 , 746 and 897 cm^{-1} . The peaks at 746 and 897 cm^{-1} are assigned to symmetrical skeletal vibration of (CF_3)

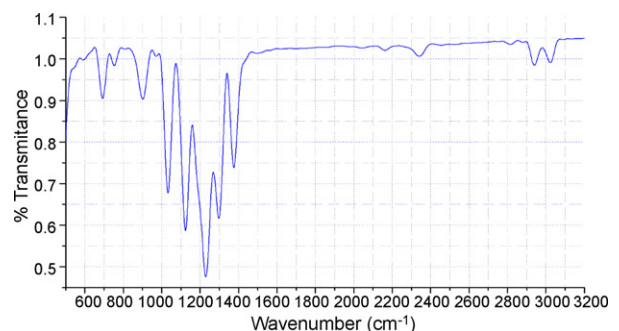


Fig. 11. FTIR spectrum of sevoflurane.

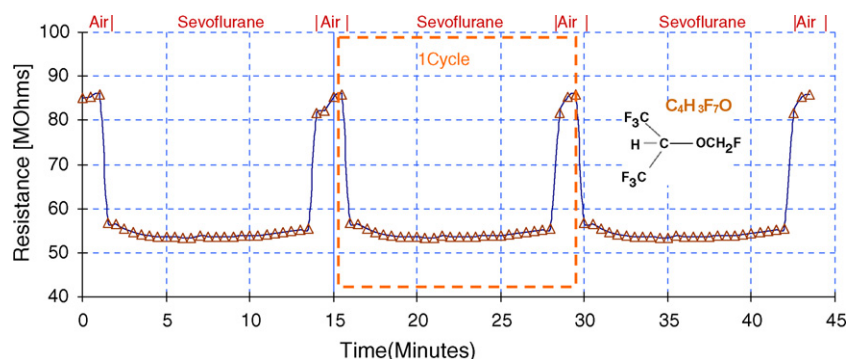


Fig. 12. Response curve for *m*-MWCNT/Ppy sensor towards 8% sevoflurane. (Inset) Structure of sevoflurane.

(CF₃)–C–O– and CH₂ rocking vibration, respectively. The IR band at 1033 cm⁻¹ is due to the C–F stretch, the –C–O stretch is seen at 1123 and the 1230 cm⁻¹ peak is due to asymmetric C–O–C stretching vibration mainly attributed to CH₂ rocking vibration. The band at 1378 cm⁻¹ could be also from CHF₃ stretching. The –CH₂–O stretch is seen at 2819 cm⁻¹. The less conspicuous aliphatic –CH bending vibration is seen between 1410 and 1420 cm⁻¹. Aliphatic –CH stretching, ν_{CH} and –CH₂ stretching, ν_{CH_2} are seen at 2878 and 2945 cm⁻¹. The –CH₂ stretching is less prominent along with other peak in the region of 3025 cm⁻¹. The aliphatic –CH stretching, ν_{CH} at 3300 cm⁻¹ has not been observed may be due to the presence of more bulky atoms around that influencing the ν_{C-H} stretch. The measured FTIR spectrum of sevoflurane vapor was subjected to baseline correction and after involving appropriate smoothing techniques is shown as Fig. 11.

4.3. Sensor response to sevoflurane

Fig. 12 plots the typical response curve of the gas sensors during sensing at room temperature. Also the figure shows, when the sensor was exposed to sevoflurane gas, the measured resistance, R_m (Ω) for each cyclic test. The response curve shows that the resistance signal varies with time over a series of cyclic test. Each cyclic test was marked over the graph. The concentration of sevoflurane used here was 8%. Prior to each cyclic test, the sensor was exposed to air and the measured resistance R_m is almost equal to R_{air} . In the beginning of each cyclic test, a specified concentration of sevoflurane say 8% was pumped into the glass chamber. The change in resistance R_m was measured. With customary on and offs, the sevoflurane concentration was passed into the glass chamber at regular intervals, only to see the change in corresponding resistance as given in the plot. This change in resistance signal was stable with high repeatability. Measurements were also taken while the sevoflurane concentration was low. With the concentration of sevoflurane, 150 ppm, the sensor response was about 1.1 (resistance of sensor upon sevoflurane was 57.2 M Ω) and the ratio of signal to noise (S/N) of the baseline was about 3.

4.4. Sensor response time

The time to achieve a steady-state response after switching gas concentrations is said to be the response time of the sensor,

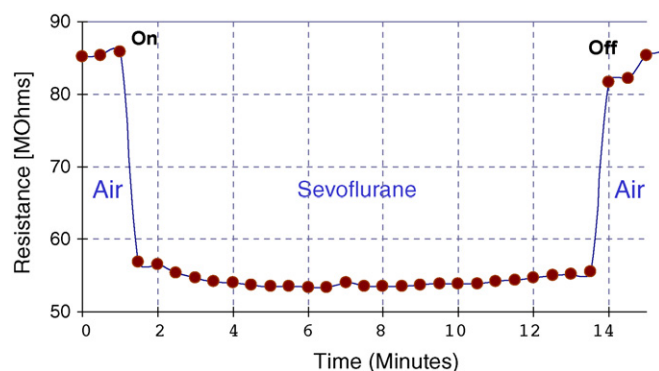


Fig. 13. Signal response when switched back and forth from sevoflurane to air used to calculate the response time, t_R .

t_R . The response time for sevoflurane detection is determined from Fig. 13 and was found to be constant all through the measurement, slightly varied with chip ± 5 s to the chip that was due to inconsistency in thin film thickness and also due to the variation in experimental temperature ± 3 °C. In some cases, operation at slightly higher elevated temperatures improved the response time of the sensor as it is cycled between dry and humid environments. The response time, t_R , was calculated to be approximately 75 s, indicating signal response of sevoflurane to air or vice versa.

5. Conclusion

An active wireless system for sensing volatile organic compounds has been designed and developed. The developed compact wireless, active RF (433 MHz) powered sensor based on *m*-MWCNTs/Ppy was used for the measurement of anesthetic agent sevoflurane, 2,2,2-trifluoro-1-(trifluoro methyl) ethyl ether at room temperature. Sensor works based on the change in resistance or voltage of the composite film sensor when exposed to the target gases. The responses of the wireless composite film sensor for other volatile analytes (C₂H₅OH, CH₃COCH₃) were also measured. The integrated architecture appears practical for sensing volatiles.

This work has proposed a scheme to develop a wireless integrated chemical sensor for volatiles. Any chemical sensor chip can easily be adopted with this smart transmitting scheme to realize a wireless sensor network system. This system is not

just for indoor environments, but can be used outdoor as well. The wireless sensing system is capable of sensing and transmitting the information to a remote monitoring system or a network. This technology smoothes the way for the future development of self-powered wireless sensing systems to be rapidly and inexpensively deployed either in hazardous environments or industrial settings with high-performance levels. If the integrated chemical sensor chip is equipped with an RF modem that enables a single unit or a networked system of units to communicate on a real-time basis within a certain range enabling real time wireless monitoring system.

Acknowledgements

We thank all the members of the Gas Metrology Group [G300], Center for Measurement Standards/National Measurement Laboratory, ITRI and Mr. Michael F. Huang, Chairman & General Manager and the members of U-CAN DynaTex Inc., Nankang Industrial Park, Nantou City, Taiwan for letting us utilize the facilities. Authors, THL & SLH would like to acknowledge the National Science Council (NSC) of Taiwan, ROC for the financial support to Department of Civil Engineering, National Chiao Tung University (NCTU), Taiwan in the form of a research project, Grant no. NSC95-2221-E-009-241-MY3. Authors, MC and RJW express thanks to Dr. B.Y. Wei of MCL/ITRI, Taiwan for kindly supplying us with the necessary MWCNTs as and when required.

References

- [1] T.K. Hamrita, E.C. Hoffacker, Development of a "smart" wireless soil monitoring sensor prototype using RFID technology, *Appl. Eng. Agric.* 21 (2005) 139–143.
- [2] A. Mulchandani, *Chemical and Biological Sensors for Environmental Monitoring*, Oxford University Press, 2000.
- [3] Available online at: http://www.eere.energy.gov/industry/sensors_automation/news_detail.html/news_id=9621.
- [4] T.C. Chen, RFID and sensor-based container content visibility and seaport security monitoring system, *Proc. SPIE: Int. Soc. Opt. Eng.* 5778 (Part I) (2005) 151–159.
- [5] M.K. Jain, C.A. Grimes, A wireless magneto-elastic micro-sensor array for simultaneous measurement of temperature and pressure, *IEEE Trans. Magn.* 37 (2001) 2022–2024.
- [6] N. Cho, S.-J. Song, S. Kim, S. Kim, H.-J. Yoo, A 5.1- μ W UHF RFID tag chip integrated with sensors for wireless environmental monitoring, in: *Proceedings of the ESSCIRC*, Grenoble, France, 2005.
- [7] B.A. Warneke, K.S.J. Pister, An ultra-low energy microcontroller for smart dust wireless sensor networks, *IEEE Int. Solid-State Circuits Conf. Dig. Tech. Papers*, 2004, pp. 316–323.
- [8] H. Yu, K. Najafi, Low-power interface circuits for bio-implantable microsystems, *IEEE Int. Solid-State Circuits Conf. Dig. Tech.* 1 (2003) 194–487.
- [9] C.C. Lu, C.S. Tsai, S.T. Ho, C.M. Chueng, J.J. Wang, C.S. Wong, S.Y. Chang, C.Y. Lin, Pharmacokinetics of desflurane uptake into the brain and body, *Anaesthesia* 59 (2004) 216–221.
- [10] W.M. Ho, W.T. Hung, C.C. Wu, C.H. Shen, N.C. Yang, K.L. Hwang, K.C. Wong, Application of MVBC equation to predict mixed venous blood concentrations of sevoflurane in cardiac anesthesia, *Anaesthesia* 60 (2005) 882–886.
- [11] F. Kevin, AANA journal course: update for nurse anesthetists—occupational exposure to trace anesthetics: quantifying the risk, *J. Am. Assoc. Nurse Anesth.* 61 (1993) 4.
- [12] K. Saito, T. Takayasu, J. Nishigami, T. Kondo, M. Ohtsuji, Z. Lin, T. Ohshima, Determination of the volatile anesthetics halothane, enflurane, isoflurane, and sevoflurane in biological specimens by pulse-heating GC–MS, *J. Anal. Toxicol.* 19 (1995) 115–119.
- [13] N.C. Yang, K.L. Hwang, C.H. Shen, H.F. Wang, W.M. Ho, Simultaneous determination of fluorinated inhalation anesthetics in blood by gas chromatography–mass spectrometry combined with a headspace autosampler, *J. Chromatogr. B* 759 (2001) 307–318.
- [14] P.D. Levin, D. Levin, A. Avidan, Medical aerosol propellant interference with infrared anaesthetic gas monitors, *Br. J. Anaesth.* 92 (2004) 865–869.
- [15] S. Floate, C.E.W. Hahn, Electrochemical reduction of the anaesthetic agent sevoflurane in the presence of oxygen and nitrous oxide, *Sens. Actuators B: Chem.* 99 (2004) 236–252.
- [16] M. Buratti, C. Valla, D. Xaiz, G. Brambilla, A. Colombi, Determination of hexafluoroisopropanol a sevoflurane urinary metabolite by 9-fluorenylmethyl chloroformate derivatization, *J. Chromatogr. B* 776 (2002) 237–243.
- [17] A.L. Cholli, C. Huang, V. Venturella, D.J. Pennino, G.G. Vernice, Detailed investigation of sevoflurane and its degradation products. Part II. Two-dimensional fluorine-19 NMR characterization of sevoflurane, *Appl. Spectrosc.* 43 (1989) 24–27.
- [18] A. Branca, P. Simonian, M. Ferrante, E. Novas, R.M. Negri, Electronic nose based discrimination of a perfumery compound in a fragrance, *Sens. Actuators B: Chem.* 92 (2003) 222–227.
- [19] M.C. Lonergan, E.J. Severin, B.J. Doleman, S.A. Beaber, R.H. Grubbs, N.S. Lewis, Array-based vapor sensing using chemically sensitive carbon black-polymer resistors, *Chem. Mater.* 8 (1996) 2298–2312.
- [20] J.M. Slater, E.J. Watt, An examination of ammonia poly(pyrrole) interactions by piezoelectric and conductivity measurements, *Analyst* 116 (1991) 1125–1130.
- [21] J.W. Grate, S.J. Martin, R.M. White, Acoustic-wave microsensors 1, *Anal. Chem.* 65 (1993) A940–A948.
- [22] H.V. Shurmer, P. Corcoran, J.W. Gardner, Integrated arrays of gas sensors using conducting polymers with molecular-sieves, *Sens. Actuators B: Chem.* 4 (1991) 29–33.
- [23] B. Li, G. Sauv e, M.C. Iovu, M.J. -EL, R. Zhang, J. Cooper, S. Santhanam, L. Schultz, J.C. Revelli, A.G. Kusne, T. Kowalewski, J.L. Snyder, L.E. Weiss, G.K. Fedder, R.D. McCullough, D.N. Lambeth, Volatile organic compound detection using nanostructured copolymers, *Nano Lett.* 6 (2006) 1598–1602.
- [24] K. Potje-Kamloth, Chemical gas sensors based on organic semiconductor polypyrrole, *Critical Rev. Anal. Chem.* 32 (2002) 124–140.
- [25] M.M. Chehimi, M.L. Abel, C. Perruchot, M. Delamar, S.F. Lascelles, S.P. Armes, *Synthetic Met.* 104 (1999) 51–59.
- [26] B. Saoudi, C. Despas, M.M. Chehimi, N. Jammul, M. Delamar, J. Bessiere, A. Walcarius, *Sens. Actuators B* 62 (2000) 35–42.
- [27] A. Azioune, F. Siroti, J. Tanguy, M. Jouini, M.M. Chehimi, B. Miksa, S. Slomkowski, *Electrochim. Acta* 50 (2005) 1661–1667.
- [28] V.G. Khomenko, V.Z. Barsukov, A.S. Katashinskii, *Electrochim. Acta* 50 (2005) 1675–1688.
- [29] N.T.L. Hien, B. Garcia, A. Pailleret, C. Deslouis, *Electrochim. Acta* 50 (2005) 1747.
- [30] L. Torsi, M. Pezzuto, P. Siciliano, R. Rella Sabbatini, L. Valli, P.G. Zambonin, Conducting polymers doped with metallic inclusions: new materials for gas sensors, *Sens. Actuators B: Chem.* 48 (1998) 362–367.
- [31] C.P. Melo, B.B. Neto, E.G. Lima, L.F.B. Lira, J.E.G. Souza, Use of conducting polypyrrole blends as gas sensors, *Sens. Actuators B: Chem.* 109 (2005) 348–354.
- [32] J. Kong, N.R. Franklin, C. Zhou, M.G. Chapline, S. Peng, K. Cho, H. Dai, Nanotube molecular wires as chemical sensors, *Science* 287 (2000) 622–625.
- [33] R.H. Baughman, C. Cui, A.A. Zakhidov, Z. Iqbal, J.N. Barasci, G.M. Spinks, G.G. Wallace, A. Mazzoldi, D. de Rossi, A.G. Rinzler, O. Jaszchinski, S. Roth, M. Kertesz, Carbon nanotube actuators, *Science* 284 (1999) 1340–1342.
- [34] J. Fan, M. Wan, D. Zhu, B. Chang, Z. Pan, S. Xie, Synthesis, characterizations, and physical properties of carbon nanotubes coated by conducting polypyrrole, *J. Appl. Polym. Sci.* 74 (1999) 2605–2610.

- [35] Q. Ameer, S.B. Adeloju, Polypyrrole-based electronic noses for environmental and industrial analysis, *Sens. Actuators B: Chem.* 106 (2005) 541–552.
- [36] M.D. Hsieh, E.T. Zellers, In situ UV-photopolymerization of gas-phase monomers for microanalytical system applications, *Sens. Actuators B: Chem.* 82 (2002) 287–296.
- [37] P. Rapta, R. Faber, L. Dunsch, A. Neudeck, O. Nuyken, In situ EPR and UV-vis spectroelectrochemistry of hole-transporting organic substrates, *Spectrochim. Acta Part A* 56 (2000) 357–362.
- [38] Y. Shen, M. Wan, In situ doping polymerization of pyrrole with sulfonic acid as a dopant, *Synthetic Met.* 96 (1998) 127–132.

Biographies

Murthy Chavali received his M.Sc. (Technology) in Chemistry (1994) from Jawaharlal Nehru Technological University, India and Ph.D. Technology (2000) from Technische Universität Wien, Austria in analytical chemistry and served as a postdoctoral scientist at Center for Instrumental Analysis, Kobe University, Japan, with Japanese National Scientific Fellowship (JSPS) supporting his research on NIR combustion sensors. Later he joined as a researcher for a short period at Precision Instrument Development Center (PIDC—now Instrument Technology Research Center, ITRC), under National Science Council (NSC), Taiwan R.O.C and moved to CMS/ITRI, Taiwan, in 2003 as a researcher in Sensors and Standards Group. Presently he is with private industry as R&D In-charge for Chemical Section. His research interests are optical waveguide technology, IR sensors, LIF, chip-based chemical and biochemical sensors (μ & η), development and application of spectroscopic techniques for the study of nanomaterials. His present research focuses on synthesis and fabrication of various organic, inorganic nanostructured materials, composites and nanosen-

sor array technology, broadly, nanotechnology applications for gas and liquid sensors.

Tzu-Hsuan Lin finished his M.Sc. (Technology) in Civil Engineering in 2003 from National Chiao Tung University, Taiwan, Republic of China; currently he is pursuing for his doctoral degree at the Department of Civil Engineering, NCTU, where he is responsible for the development of smart sensors, wireless networks, RFID technology for health of structures and building risk monitoring.

Ren-Jang Wu working as an assistant professor at Department of Applied Chemistry, Providence University, Taiwan, Republic of China. He received B.S. in chemistry from National Tsing Hua University in 1986, and M.S. in chemistry from National Taiwan University in 1988 and a Ph.D. in chemistry from National Tsing Hua University in 1995. His main areas of interest are chemical sensors, catalysis, chemical standard technology and nanoscience.

Hsiang-Ning Luk currently is the Chairman of the Department of Anesthesiology, Taichung Veterans General Hospital, Taiwan. He received his M.D. and M.S. from National Defense Medical Center, Taipei, Taiwan and Ph.D. from the Department of Physiology, Leuven University, Belgium. Presently he is an associate professor, Department of Applied Mathematics, Providence University, Taiwan. His research interests are pharmacodynamics and pharmacokinetics of anesthetics.

Shih-Lin Hung received his M.S. (1990) and Ph.D. (1992) from The Ohio State University in 1990 and 1992. He is currently a chair professor in the Institute of Civil Engineering at National Chiao Tung University, Taiwan, Republic of China. His main research interests include areas like expert systems, ANN, machine learning, parallel computing, CAE wireless sensor networks, structural health monitoring and wavelet.